

# International Journal of Advance Research in Engineering, Science & Technology

e-ISSN: 2393-9877, p-ISSN: 2394-2444 **Volume 5, Issue 5, May-2018** 

# Texture Analysis of Thyroid Ultrasonography Images for Diagnosis of Benign & Malignant Nodule Using Feed Forward Neural Network

Shrikant D. Kale<sup>1</sup>, Akash R. Dudhe<sup>2</sup>

<sup>1,2</sup>Assistant Professor, Electronics & Telecommunication Engineering Department, <sup>1,2</sup> Jagadambha College of Engineering & Technology, Yavatmal, Maharashtra, India. <sup>1</sup>shrikant\_kale97@rediffmail.com, <sup>2</sup>akash.dudhe@gmail.com

Abstract — A texture analysis of medical images gives the quantitative information about the tissue characterization & internal structure of organs for possible pathology. The physician deducing the useful information concerning internal body parts for the pathology or lesions. This is the till subjective matter of concern & thus to provide the objectification of disease diagnosis from the medical image, this paper gives the idea for thyroid nodule diagnosis using texture of the ultrasound images. Thyroid gland is located at the base of the neck, just below Adam's apple which produces hormones that control body metabolism. The nodules are found in thyroid may be benign or malignant. In this paper, gray level co-occurrence matrix (GLCM) is used as the texture characterization technique. The 10 GLCM feature are selected for feature extraction & GLCM matrix is calculated for four different orientation & different pixel distance from 1 to 15. The extracted features are classified using feed forward network using Levenberg-Marquardt backpropagation optimized training algorithm for diagnosis of thyroid nodule malignancy risk. The experimental results show the performance measure of feed forward neural network in terms classification accuracy, Positive predicted rate, Negative predicted rate, sensitivity & specificity.

Keywords- Texture Analysis; Thyroid Nodule; GLCM; Feed Forward Neural Network.

## I. INTRODUCTION

A thyroid is small gland located at the base of the neck, just below the Adam's apple. It is butterfly shaped with two cones like lobes on either side. Thyroid gland produces the T3 & T4 hormones, which control the rate of many activities in the body. One of the common disorders of thyroid gland is the occurrence of the thyroid nodule. The thyroid nodule can be solid mass, cysts which either benign (non-cancerous) or malignant (cancerous) [1]. A National Cancer Registry program (NCRP) maintains the reliable data of cancer patient on the magnitude & pattern of cancer in India. The projection of thyroid cancer cases in year of 2010 is around 16,215 & by the year of 2020 goes up to 19,113. The cases of malignant thyroid nodule are found to be more in female to that of male. The projection of thyroid cancer in female for year of 2010, 2015 & 2020 is 11,751; 12,808 & 13,955 significant over male i.e. 4,464; 4,798 & 5,158 for the respective years [3]. The other figures of thyroid disease are turn out to be 42 million in the Indian context from the projection of various studies on thyroid diseases [2].

All radiological modalities like ultrasound, CT, Scintigraphy, SPECT, MR, PET, X-rays etc. play an important role in process of disease diagnosing and have become major evidence to ensure disease. The preferred diagnosis method used for possible lesions are ultrasonography. Because as ultrasound (US) possesses a rare combination of advantages including portability, invasive, real-time data acquisition and affordability [4]. Ultrasonography is a diagnostic imaging tool used to visualize subcutaneous body structures and internal organs. The physicians are deducing useful information concerning the tissue characterization and structure. Thus, Ultrasonography has become an invaluable tool for the accurate diagnosis and follows up of different pathologies in a variety of tissues and organs [5].

The detection of the pathological diseases such as thyroid nodule by physicians is still subjective matter & while making manual diagnosis from images, some relevant information need not to be recognized by human visual system. In the suspicious cases FNA, Cytological test are done to find the malignancy risk in thyroid gland nodule. Thus to provide the objectification for thyroid nodule disease diagnosis the various texture characterization techniques are utilized which draws statistical information from Ultrasonography image. Thus this texture quantitative information is used to classify into benign & malignant thyroid nodule.

# II. RELATED WORK

There have been various attempts towards the subjective techniques for diagnosis of thyroid gland nodule. Some of the earlier research for thyroid nodule diagnosis is described. In <sup>[4]</sup>, the 13 GLCM texture & geometric features extracted from thyroid images by region based active contour segmentation method & classified using SVM, KNN and Bayesian <sup>[4]</sup>

In <sup>[5]</sup>, the Contour let Transform (CT) using LP and DFB filters to the 3rd level decomposition are used for detection hypoechoic and isoechoic nodules from normal thyroid nodule. A Gaussian kernel SVM classifier is applied along the SFFS algorithm with or without coefficient thresholding. In <sup>[6]</sup>, the texture features based on the CT using different types of filters banks with a selection scheme SFFS algorithm were classified by k-NN algorithm.

In [7], a novel computational approach using Radon Transform for the thyroid tissue characterization of US image were utilized. Supervised classification experimentation using KNN (k=5), SVM with polynomial kernel was done to

differentiate normal and nodular thyroid US images for detection malignancy risk. In <sup>[8]</sup>, the normal and hypoechoic nodule were classified using 2 First-order and 168 co-occurrence features drawn from manual rectangular ROI & PCA for optimal subset using Binary Logistic Regression.

In <sup>[9]</sup>, a novel approach that correlates thyroid malignancy, LBP, FLBP, and FLGH Ultrasound texture features which discriminated by SVM with linear, polynomial and Gaussian kernel with or without fusion of texture using 10 fold cross validation or 1 way ANOVA. In <sup>[10]</sup>, a novel fuzzy feature extraction method (FLBP). The FLBP approach was experimentally evaluated using supervised SVM with linear, polynomial, radial basis, sigmoid kernel for classification of nodular and normal thyroid US images. In <sup>[11]</sup>, the joint texture analysis on US and Cytological images were processed to optimally highlight the cancerous region in same image. The 20 textural features were generated which contain 4 GH, 10 GLCM and 6 RLM from US image. 20 morphological and textural features were extracted from segmented nuclei of Cytological image. An SVM classifier with 2nd degree polynomial kernel & Bayesian with quadratic kernel were used in distinguishing correctly low from high-risk thyroid nodules.

#### III. MATERIAL & METHOD

Medical ultrasound images of thyroid gland are selected for texture analysis in experimental work. These ultrasound images contained some of abnormal images having benign thyroid nodule (non-cancerous) and malignant thyroid nodule (cancerous). The total 85 thyroids ultrasound images were used which contains total 48 cancerous and 37 non-cancerous nodules was selected in database. These thyroid images are available in image gallery of Wilmington Endocrinology PA on website. The image size of  $546 \times 410$ , with 24 bit depth size, true color image, format of images are JPEG.

The Matlab R2010a software utilizing image processing toolbox & neural network toolbox are used for experimental work. The preprocessing steps required for the texture analysis is gray scale conversion of true color image & then image resizing into 256×256. Then GLCM texture feature extraction & classification of texture feature are carried out & described in following section.

#### 3.1 Texture Analysis Method:

The texture features analysis is a useful way of increasing the quantitative information obtains from medical images. It is an ongoing field of research, with applications ranging from the segmentation of specific anatomical structures and the detection of lesions, to differentiation between pathological and healthy tissue in different organs. Texture analysis uses radiological images obtained in routine diagnostic practice, but involves an ensemble of mathematical computations performed with the data contained within the images <sup>[12]</sup>.

According to the methods employed to evaluate the inter-relationships of the pixels, the forms of texture analyses are categorized as structural, model-based, statistical and transform methods <sup>[13]</sup>.

#### 3.1.1 Statistical Methods

These are based on representations of texture using properties governing the distribution and relationships of grey-level values in the image & normally achieve higher discrimination indexes than the structural or transform methods <sup>[12]</sup>.

### 3.2 Texture Feature Extraction Methods

Medical images possess a vast amount of texture information relevant to clinical practice. For example, US images of tissues are not capable of providing microscopic information that can be assessed visually. However, histological alterations present in some illnesses may bring about texture changes in the US image that are amenable to quantification through texture analysis. This has been successfully applied to the classification of pathological tissues from the liver, thyroid, breasts, kidneys, prostate, heart, brain and lungs [12].

The most commonly used texture features are Gray Level Histogram, Run-length matrix, Gray Level Co-occurrence matrix, contour let transform, Wavelets transform, Radon Transform, Local Binary Pattern, Fuzzy Local Binary Pattern, Fuzzy local Gray Histogram.

These texture feature found in literature of texture analysis on ultrasound medical images of thyroid gland for detection of thyroid nodule as a benign or malignant tissue from normal one. In this paper, gray level co-occurrence matrix (GLCM) based texture feature extraction approach is fallowed which explain next in detail. The ten texture features extracted from GLCM are described mathematically next section 3.2.1.

# 3.2.1 Gray Level Co-Occurrence Matrix

Using histograms in calculation will result in measures of texture that carry only information about distribution of intensities, but not about the relative position of pixels with respect to each other in that texture. Using a statistical

approach such as co-occurrence matrix will help to provide valuable information about the relative position of the neighboring pixels in an image.

Given an gray scale image I, of size N×N, the co-occurrence matrix P can be defined as

$$P(i,j) = \sum_{x=1}^{N} \sum_{y=1}^{N} \begin{cases} 1 \ ; I(x,y) = i \text{ and } I(x + \Delta x, y + \Delta y) = j \\ 0 \ ; \text{otherwise} \end{cases}$$
 (1)

Here, the offset  $(\Delta x, \Delta y)$ , is specifying the distance between the pixel-of-interest and its neighbor. Note that the offset  $(\Delta x, \Delta y)$  parameterization makes the co-occurrence matrix sensitive to rotation. Choosing an offset vector, such that the rotation of the image is not equal to 180 degrees, will result in a different co-occurrence matrix for the same (rotated) image. This can be avoided by forming the co-occurrence matrix using a set of offsets sweeping through 180 degrees at the same distance parameter  $\Delta$  to achieve a degree of rotational invariance (i.e.,  $[0 \ \Delta]$  for 0 degree: P horizontal,  $[-\Delta, \Delta]$  for 45 degree: P right diagonal,  $[-\Delta, 0]$  for 90 degree: P vertical, and  $[-\Delta, \Delta]$  for 135degree: P left diagonal).

The GLCM matrix computed from the thyroid gland ultrasound images are of the size 256×256. Then texture features were extracted from GLCM matrix from each of the thyroid gland ultrasound image database & the mathematical equations for the texture features are given as follows:

| C                      |  |      |
|------------------------|--|------|
| Autocorrelation        | $\sum_{i}\sum_{j}(i.j)P(i,j)$  | (2)  |
| Contrast               | $\sum_{i} \sum_{j}  i - j ^2 P(i, j)$  | (3)  |
| Correlation            | $\sum_{i} \sum_{j} \frac{(i-\mu x) \cdot (j-\mu y) P(i,j)}{\sigma x \cdot \sigma y}$ | (4)  |
| Cluster Prominence     | $\sum_{i} \sum_{j} (i + j - \mu x - \mu y)^{4} P(i, j)$                              | (5)  |
| Cluster Shade          | $\sum_{i} \sum_{j} (i + j - \mu x - \mu y)^{3} P(i, j)$                              | (6)  |
| Dissimilarity          | $\sum_{i} \sum_{j}  i-j  P(i,j)$   | (7)  |
| Energy                 | $\sum_{i} \sum_{j}  P(i,j) ^2$   | (8)  |
| Entropy                | $-\sum_{i}\sum_{j}P(i,j)\log(P(i,j))$  | (9)  |
| Homogeneity            | $\sum_{i} \sum_{j} \frac{P(i,j)}{1+ i-j }$   | (10) |
| Maximum<br>Probability | $\max_{i,j} P(i,j)$  | (11) |

Notation & expression used for calculating the GLCM statistics are as shown below.

| Notation               | Meaning   |      |
|------------------------|---|------|
| μx                     | $\sum_{i} \sum_{j} i \cdot P(i, j)$               | (12) |
| μy                     | $\sum_{i} \sum_{j} j \cdot P(i, j)$               | (13) |
| $\sigma_{\rm x}^{\ 2}$ | $\sum_{i} \sum_{j} (\; i - \mu_x)^2 \; .  P(i,j)$ | (14) |
| $\sigma_{\rm y}^{\ 2}$ | $\sum_{i} \sum_{j} (j - \mu_{y})^{2}$ . $P(i, j)$ | (15) |

The above motioned ten features extracted 85 image database are utilized for feature classification. The feature classification is done to identify the malignant thyroid nodule from that of benign thyroid nodule. The classification method used in evaluation is described in next section.

#### 3.3 Classification Method

The experimental evaluation of GLCM texture features extracted from ultrasound thyroid gland images was classified by feed forward neutral network. It is a two-layer feed-forward network, with differential sigmoid transfer function in hidden neuron layer and linear transfer function in output neurons layer & Gradient descent weight and bias learning function is utilized for updating the weights. It can classify vectors arbitrarily well for a given enough neurons in its hidden layer.

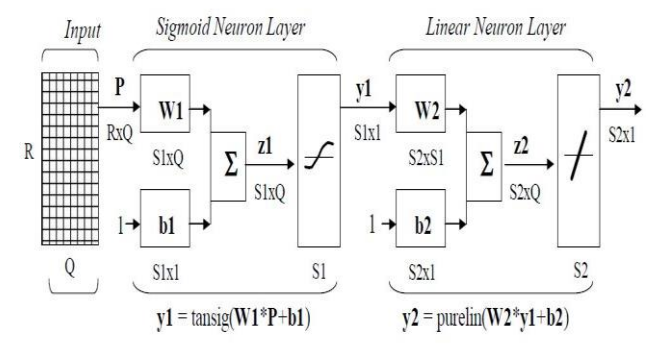


Figure 1. A two layer feed forward neural network.

The fig 1 shows the two layer feed forward network, the input layer with Q neurons are supplied with texture feature vectors having Q representative R elements. The numbers of neuron in hidden layer are adjusted as desired to get accurate results. In the hidden layer Si neurons are connected to the input layer Q neurons by weight W1. Therefore the weight vector W1 connecting input & hidden layer neurons of size Si×O.

The net input at hidden layer is calculated as

$$z1 = \sum W1 * P + b1 \tag{16}$$

Where, P is the input to the input layer neurons

W1 is the weight between input & hidden layer

b1 is the bias to the hidden layer neurons

The output of the hidden layer Y1 is calculated as

$$Y1 = tansig(z1) (17)$$

The tan sigmoid transfer function is utilized in hidden layer to calculate a hidden layer's output from its net input & mathematical equation of tan sigmoid transfer function is

$$tansig(z1) = \frac{2}{1 + e^{-2z_1}} - 1 \tag{18}$$

The output layer has N neurons depending on classes of the problem as in our case; there are two classes such as benign nodule & malignant nodule. Y1 is the input to the output layer neurons. The hidden layer Si neurons is connected to the output layer neurons Sj by weight W2 & bias b2, where size of weight matrix is Sj×Si. The net input at output layer is calculated as

$$z2 = \sum W2 * Y1 + b2 \tag{19}$$

Where, Y1 is the input to the input layer neurons

W2 is the weight between hidden & output layer

B2 is the bias to the output layer neurons

The output of the output layer Y2 is calculated as

$$Y2 = purelin(z2) \tag{20}$$

The pure linear transfer function is utilized in output layer to calculate a layer's output from its net input.

### 3.4.1 Gradient Descent Algorithm with momentum Term

Mean Square Error is used as an error function to calculate the error at each iteration using the target output & the final calculated output of the learning at each iteration. If the error is still larger than the predefined acceptable error value, the training process continues to the next iteration [14].

$$E = \frac{1}{2}\sum (T - y^2)^2 \tag{21}$$

 $E = \frac{1}{2}\sum (T - y2)^2$  (21)
For weight associated to each connection link between output layer to hidden layer, the weight incremental value is computed using a weight adjustment equation as follows [14].

$$\Delta W_2(t) = -\eta \frac{dE}{dW_2} + \mu \Delta W_2(t-1) \tag{22}$$

Where, η learning parameter

μ Momentum parameter

 $\Delta W_2$  (t) Change in weight for t<sup>th</sup> iteration

Gradient descent with momentum, implemented by allows a network to respond not only to the local gradient, but also to recent trends in the error surface. Without momentum a network can get stuck in a shallow local minimum. With momentum a network can slide through such a minimum.

Gradient descent with momentum depends on two training parameters. The parameter  $\eta$  indicates the learning rate, similar to the simple gradient descent. The parameter  $\mu$  is the momentum constant that defines the amount of momentum.  $\mu$  is set between 0 (no momentum) and values close to 1 (lots of momentum) [14].

# 3.4.2 Levenberg-Marquardt algorithm

The Levenberg-Marquardt algorithm was designed to approach second-order training speed without having to compute the Hessian matrix [15]. When the performance function has the form of a sum of squares, then the Hessian matrix can be approximated as

$$H = J^T . J (23)$$

& the gradient can be computed as

$$g = J^T . E (24)$$

Where J is the Jacobian matrix that contains first derivatives of the network errors with respect to the weights and biases, and E is a vector of network errors. The Jacobian matrix can be computed through a standard backpropagation technique that is much less complex than computing the Hessian matrix [15].

The Levenberg-Marquardt algorithm uses this approximation to the Hessian matrix in the following update:

$$\Delta W_2((t+1) = \Delta W_2(t) - (J^T \times J + \mu I)^{-1} \times J^T \times E \tag{25}$$

When the scalar  $\mu$  is zero, this is just using the approximate Hessian matrix. When  $\mu$  is large, this becomes gradient descent with a small step size. Thus,  $\mu$  is decreased after each successful step (reduction in performance function) and is increased only when a tentative step would increase the performance function. In this way, the performance function is always reduced at each iteration of the algorithm [15].

The parameter  $\mu_0$  is the initial value for  $\mu$ . This value is multiplied by  $\mu_{dec}$  whenever the performance function is reduced by a step. It is multiplied by  $\mu_{inc}$  whenever a step would increase the performance function. If  $\mu$  becomes larger than  $\mu_{max}$ , the algorithm is stopped <sup>[15]</sup>.

This algorithm appears to be the fastest method for training moderate-sized feed forward neural networks up to several hundred weights <sup>[15]</sup>.

#### IV. RESULTS

The two layer feed forward neural network is trained with 90% of features vector from the database & 10% of features vector is used in testing the network performance using backpropagation training with gradient descent with momentum (Levenberg-Marquardt algorithm). The dataset are prepared using the four directional orientations ( $0^0$ ,  $90^0$ ,  $45^0$ , &  $135^0$ ) & for each pixel distance starting from 0, 1... up to 15. This each dataset extracted single orientation & single pixel distance was trained & tested using backpropagation feed forward neural network. The following figure shows the training performance of backpropagation neural network for the features extracted from GLCM matrix with offset [01], means along horizontal direction with single pixel distance.



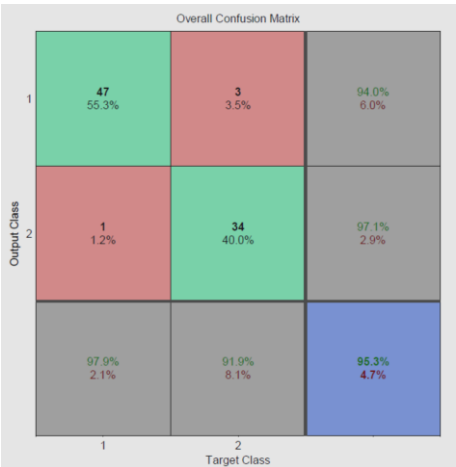


Figure 2. Performance & Confusion matrix of backpropagation neural network classifier for offset [0 1]

The fig. 2 shows the best performance of in terms of mean square error of 0.31952 at epoch 178. Then fig. 3 shows the overall confusion matrix for the same GLCM offset. The neural networks were classified malignant nodule with 97.92% accuracy & benign nodule with 91.89% accuracy. The overall accuracy of feed forward neural network classifier was 95.30%.

There are such a four instances, where the neural network has been incorrectly classified the thyroid nodule. The fig 4 shows the ROC curve for same GLCM offset, the shape of ROC curve shows the SCG backpropagation neural network has good performance.

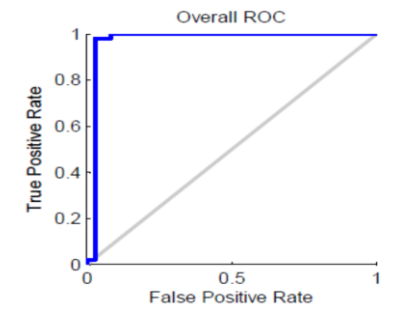


Figure 3. ROC curve for features with offset [0 1]

The table 1 shows the accuracy (Acc), positive predictive rate (PPV), negative predictive rate (NPV), Sensitivity (Se), & specificity (Sp) for the dataset trained & tested using backpropagation neural network extracted from GLCM computed in horizontal orientation with varying pixel distances.

Table 1. Performance measure of feed forward neural network classifier for feature extracted from GLCM in horizontal orientation with varying pixel distances

| Pixel<br>Distance | 1     | 2     | 3     | 4     | 5     | 6     | 7     | 8     | 9     | 10    | 11    | 12    | 13    | 14    | 15    |
|-------------------|-------|-------|-------|-------|-------|-------|-------|-------|-------|-------|-------|-------|-------|-------|-------|
| Acc (%)           | 95.29 | 98.82 | 96.47 | 95.29 | 98.82 | 97.65 | 96.47 | 97.65 | 96.47 | 97.65 | 97.65 | 97.50 | 95.29 | 97.65 | 96.47 |
| PPV<br>(%)        | 97.92 | 97.92 | 95.83 | 97.92 | 97.92 | 100   | 97.92 | 95.83 | 93.75 | 95.83 | 95.83 | 95.83 | 97.92 | 97.92 | 97.92 |
| NPV<br>(%)        | 91.89 | 100   | 97.30 | 91.89 | 100   | 94.59 | 94.59 | 100   | 100   | 100   | 100   | 100   | 91.89 | 97.30 | 94.59 |
| Se (%)            | 94.00 | 100   | 97.87 | 94.00 | 100   | 96.00 | 95.92 | 100   | 100   | 100   | 100   | 100   | 94.00 | 97.29 | 95.92 |
| Sp (%)            | 97.14 | 97.37 | 94.74 | 97.14 | 97.37 | 100   | 97.22 | 94.87 | 92.50 | 94.87 | 94.87 | 94.87 | 97.14 | 95.92 | 97.22 |

The following figure shows the performance measure of feed forward neural network as mean over the entire pixel distances in each directional orientation.

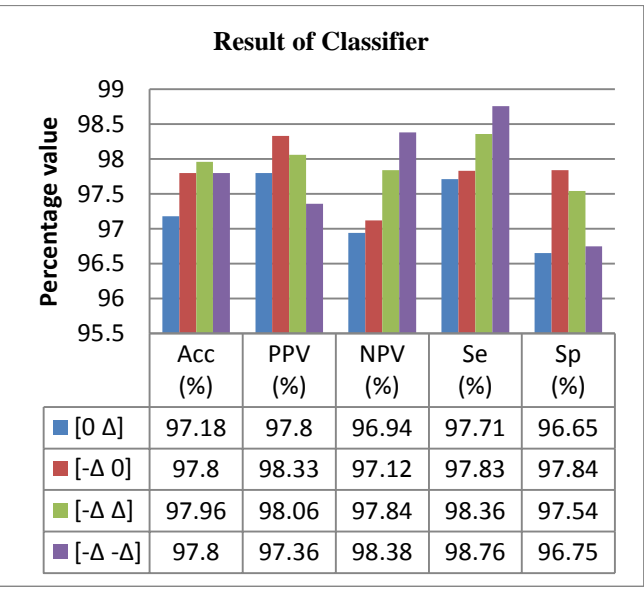


Figure 4. Performance measure of feed forward neural network calculated as the mean over the pixel distance for each orientation.

# V. CONCLUSIONS

Texture analysis of ultrasound medical images using quantitative information of the tissue characterization is used for the detection of thyroid nodule. The 10 gray level co-occurrence based texture features being extracted from 37 benign and 48 malignant thyroid images are use to classify into risk of malignancy using two layer feed forward neural network with gradient descent backpropagation with momentum term (Levenberg-Marquardt algorithm) with ten neurons in hidden layer. The tan sigmoid & pure linear transfer functions are utilized in hidden & output layer respectively with minimum gradient of 1 e<sup>-10</sup> & initial  $\mu$  of 0.001,  $\mu$  decrement factor of 0.1,  $\mu$  increment factor of 10 &  $\mu$  maximum is taken as 1 e<sup>10</sup>. The performance of classifier shows the classification accuracy of 97.69  $\pm$  1.44 %. This classifier accuracy is calculated as mean of accuracies mentioned in chart 1 of performance measure of classifier. Thus, it's providing the objective method to physician to diagnosis of thyroid gland ultrasound images for detection of nodules malignancy risk. The classification of benign & malignant nodule will provide the second opinion to the physician about treatment of patient's and thus, the proposed work will help the physician to minimize the misdiagnosis rate of pathological diseases.

#### REFERENCES

- [1] Eystratios G. Keramidas, Dimitris K. et al, "Efficient and effective ultrasound image analysis scheme for thyroid nodule detection", Lect. Notes Computer Science 4633:pp 1052–1060, 2007.
- [2] Ambika G. Unnikrishnan, Usha V. Menon, "Thyroid disorders in india: A epidemiological perspective", Indian Journal of Endocrinology and Metabolism, vol. 15, suppliment 2, pp 78-81, 2011.
- [3] Ramnath Takiar, Deenu Nadayil, A Nandakumar: "Projections of Number of Cancer Cases in India (2010-2020) by Cancer Groups", Asian Pacific Journal of Cancer Prevention, Vol. 11, pp. 1045-1049, 2010.
- [4] Nikita Singh, Alka Jindal, "A Segmentation Method and Comparison of Classification Methods for Thyroid Ultrasound Images", International Journal of Computer Applications (0975 8887) Volume 50 No.11, pp 43-49, July 2012.
- [5] Stamos Katsigiannis, Eystratios G. et al, "A Contourlet Transform Feature Extraction Scheme for Ultrasound Thyroid Texture Classification", Engineering Intelligent Systems, Special issue: Artificial Intelligence Applications and Innovations, vol. 18, no. 3/4, 2010.
- [6] Stamos Katsigiannis, Eystratios G. et al, "Contourlet Transform for Texture Representation of Ultrasound Thyroid Images", IFIP Advances in Information & communication Technology, 339; 138-45, 2010.
- [7] M.A. Savelonasa, D.K. Iakovidis et al, "Computational Characterization of Thyroid Tissue in the Radon Domain", Twentieth IEEE International Symposium on Computer-Based Medical Systems (CBMS'07)0-7695-2905-4/07.
- [8] Maria E. Lyra, Katerina Skouroliakou et al, "Texture Characterization in Ultasonograms of the Thyroid Gland", M05-301: (10:30) NSS-MIC 2009.
- [9] Dimitris K. Iakovidis, Eystratios G. Keramidas et al, "Fusion of fuzzy statistical distributions for classification of thyroid ultrasound patterns", Artificial Intelligence in Medicine pp. 33–41, 2010.
- [10] Dimitris K. Iakovidis, Eystratios G. Keramidas et al, "Fuzzy Local Binary Patterns for Ultrasound Texture Characterization", Image Analysis and Recognition, Lecture Notes in Computer Science Vol. 5112, pp. 750-759,2008.
- [11] Stavros Tsantis, Dimitris Glotsos et al, "Improving Diagnostic Accuracy In The Classification Of Thyroid Cancer By Combining Quantitative Information Extracted From Both Ultrasound And Cytological Images", 1st International Conference "From Scientific Computing to Computational Engineering" Athens, 8-10 September, 2004.
- [12] G. Castellano, L. Bonilha et al, "REVIEW Texture analysis of medical images", Clinical Radiology 59, pp.1061–1069, 2004.
- [13] A. Materka, M. Strzelecki, "Texture Analysis Methods A Review", Technical University of Lodz, Institute of Electronics, COST B11 report, Brussels, 1998.
- [14] Kenji Suzuki, "Artificial Neural Networks Architectures And Applications", Intech open science, ISBN 978-953-51-0935-8.
- [15] Arnold Reynaldi, Samuel Lukas, et al, "Backpropagation and Levenberg-Marquardt Algorithm for Training Finite Element Neural Network", UKSim-AMSS 6th European Modelling Symposium, pp.89-94, 2012.
- [16] Shrikant D. Kale, K. M. Punwatkar, "A Different Texture Characterization Technique For Diagnosis of Thyroid Nodule Using Medical Ultrasound Images-A Survey", in Proceeding of International Conference on Emerging Trends in Technology & its Application, Karjat, Dist.Raigad, , pp. 291-297, 6-7March 2013.
  [17] Shrikant D. Kale, K. M. Punwatkar, "Texture Analysis of Ultrasound Medical Images for Diagnosis of Thyroid Nodule Using
- [17] Shrikant D. Kale, K. M. Punwatkar, "Texture Analysis of Ultrasound Medical Images for Diagnosis of Thyroid Nodule Using Support VectorMachine", International Journal of Computer Science and Mobile Computing,, ISSN: 2320–088X, Vol.2, Issue.10, pp. 71-77, October- 2013.
- [18] Shrikant D. Kale, K. M. Punwatkar, "Texture Analysis of Thyroid Ultrasound Images for Diagnosis of Benign and Malignant Nodule Using Scaled Conjugate Gradient Backpropagation Training Neural Network", International Journal of Computational Engineering & Management, ISSN: 2230-7893, Vol. 16 Issue 6, pp. 33-38, November 2013.
- [19] Shrikant D. Kale, Akash R. Dudhe, "Texture Analysis of Thyroid Ultrasound Images for Diagnosis of Cancerous Nodule Using ART1 Neural Network", International Journal of Advanced Research in Electrical, Electronics & Instrumentation Engineering, Vol. 6, Issue 4, pp. 2283-2290, April 2017. DOI:10.15662/IJAREEIE.2017.0604014